

# Interstitial Oxygen in Tin-Doped Indium Oxide Transparent Conductors

Oliver Warschekow<sup>†</sup>

School of Physics, The University of Sydney, NSW 2006, Australia

Lj. Miljacic and D. E. Ellis

Department of Physics and Astronomy, Northwestern University, Evanston, Illinois 60208

G. B. González and T. O. Mason

Department of Materials Science and Engineering, Northwestern University, Evanston, Illinois 60208

We report first-principles density functional theory calculations of interstitial oxygen in tin-doped indium oxide (ITO), a transparent conducting oxide. Interstitial oxygen plays a critical role in the defect of ITO because it is by removal of interstitial oxygen that *n*-type charge carriers are produced. The Frank and Köstlin defect model successfully rationalizes the observed conductivity, Sn-doping, and oxygen partial pressure dependencies of ITO by postulating that tin atoms, which substitute for indium, are clustered with interstitial oxygen. Structural evidence for such a clustering, however, remains ambiguous. Recently published Rietveld refinement results of X-ray and neutron diffraction data found interstitial oxygen to be significantly displaced (0.4 Å) from the ideal fourfold position. Our calculations show that the experimental position is plausible only if interstitial oxygen is clustered with  $\text{Sn}_{\text{In}}$  defects at any of the three *d*-type cation sites nearest to the interstitial, thereby providing direct structural confirmation of the Frank and Köstlin defect model.

## I. Introduction

TIN-DOPED  $\text{In}_2\text{O}_3$ , also known as indium-tin oxide (ITO), is a widely used transparent conducting oxide (TCO) with numerous applications in opto-electronics technology as transparent electrodes for flat-panel displays, electro-chromic windows, and solar panels.<sup>1,2</sup> Critical to the conducting properties of any TCO is the underlying defect chemistry and for ITO, the model of Frank and Köstlin<sup>3</sup> is now commonly referred to. Inferred from measured carrier concentrations as a function of tin-doping level and oxygen partial pressure, this model postulates that Sn (which substitutes for In) is bound in neutral defect complexes  $(2\text{Sn}_{\text{In}} \cdot \text{O}_i)^{\times}$  with interstitial oxygen. A fraction of these complexes is “reducible,” meaning that interstitial oxygen atoms can be removed under reducing conditions, freeing two *n*-type charge carriers in the process. This is in contrast to what Frank and Köstlin refer to as “non-reducible” clusters in which interstitial oxygen remains tightly bound even under highly reducing conditions.<sup>3,4</sup> While the general aspects of the Frank and Köstlin model (such as the existence of the  $(2\text{Sn}_{\text{In}} \cdot \text{O}_i)^{\times}$  clusters) are most probably correct, experiments have not been able to

provide detailed structural evidence for the formation of defect clusters. Even less is known about the relative placement of interstitial oxygen and substitutional Sn in these complexes, which is of direct relevance to the question of what distinguishes “reducible” (i.e., carrier generating) and “non-reducible” clusters from one another.

$\text{In}_2\text{O}_3$  crystallizes in the cubic bixbyite lattice (space group *Ia*3 (#206),  $a = 10.117$  Å), which contains 80 atoms or 16 formula units.<sup>5</sup> Its structure can be derived from a  $2 \times 2 \times 2$  supercell of the fluorite ( $\text{CaF}_2$ ) lattice by removing one-fourth of all anions of its simple cubic anion sub-lattice. The relative positioning of these vacant sites with respect to the center of a cube (occupied by indium) results in two types of cation sites. These are termed 8*b* and 24*d* sites (or “*b*” and “*d*” sites for short) following Wyckoff notation, and are characterized by body-diagonal and face-diagonal placement of the neighboring structural vacancies, respectively. Vacant anion sites (Wyckoff 16c) provide space to accommodate excess oxygen as interstitials. The 16c site is a special position in the *Ia*3 space group, with  $x = y = z$  as the defining criterion; this places interstitials onto an axis parallel to the [111], and we shall refer to this axis as the “16c axis.” The precise placement of interstitial oxygen on or along this axis and what it reveals about the environment of the interstitial is the concern of this article.

Interstitial oxygen is tetrahedrally coordinated by four cations, as illustrated schematically in Fig. 1. One *b*-site cation is located on the 16c axis at  $x = y = z = 0.250$  (all positions given

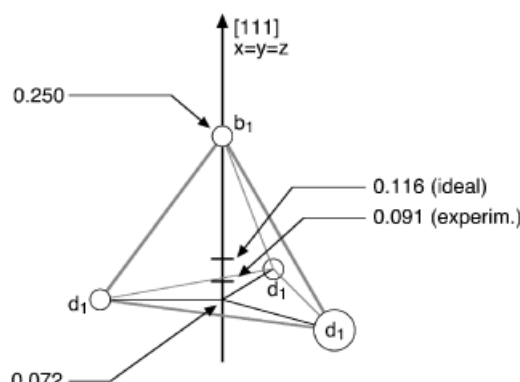


**Fig. 1.** Schematic diagram of the position of interstitial oxygen in indium-tin oxide (ITO) in lattice units along the 16c symmetry axis ( $x = y = z$ ). The four nearest cation neighbors (one *b*-site and three *d*-site cations) and the idealized interstitial position in  $\text{In}_2\text{O}_3$ , defined as the fourfold site equidistant to the four cations, are indicated. The interstitial position as reported in González *et al.*<sup>7</sup> displaced substantially (0.44 Å) from the ideal site toward the plane of *d*-site cations, is also shown.

D. Johnson—contributing editor

Manuscript No. 20156. Received February 14, 2005; approved June 28, 2005.  
This work was initiated under US DOE grant no. DE-FG02-84ER45097 and completed under NSF-MRSEC Grant no. DMR-0076097 at the Materials Research Center of Northwestern University.

<sup>†</sup>Author to whom correspondence should be addressed. e-mail: oliver@physics.usyd.edu.au

in lattice units), and three d-site cations form the base plane of the trigonal pyramid, which, in bulk  $\text{In}_2\text{O}_3$ <sup>5</sup>, intersects the 16c axis at  $x = y = z = 0.072$ . Given this geometry, an *ad hoc* estimation of the interstitial position can be arrived at by choosing the point on the axis at which the four nearest-neighbor cations are equidistant. This type of reasoning yields  $x = y = z = 0.116$ , and we will refer to this as the “ideal position.” Experimentally, the interstitial oxygen position in ITO was determined by González *et al.*<sup>6,7</sup> using Rietveld refinement of neutron and high-resolution, synchrotron X-ray diffraction data. These results found interstitial oxygen at  $x = y = z = 0.086(3)$  and  $0.091(1)$  in oxidized ITO samples containing 3 and 9 at.% Sn, respectively. This means interstitials are dramatically displaced from the “ideal” position (0.53 and 0.44 Å in absolute terms, respectively) toward the plane of nearest d cations (Fig. 1). As detailed in González *et al.*<sup>6,7</sup> the diffraction results exhibit a number of internal consistencies.  $\text{Sn}_{\text{In}}$  and  $\text{O}_i$  were found in a ratio close to 2:1 in agreement with the Frank and Köstlin model,<sup>3</sup> and no interstitial oxygen was found in pure  $\text{In}_2\text{O}_3$ . This gives us an indication that the observed interstitial displacements are genuine.

In this work, we use first-principles density functional methods to examine what may cause the observed displacement. One intriguing possibility is that the displacement is because of clustering with nearby Sn dopants. The ionic radius of Sn(IV) is approximately 0.1 Å smaller than In(III); thus, one should expect displacement of interstitials toward any site where Sn substitutes for Indium. In a diffraction experiment, which measures the (symmetry-) averaged displacement over many configurations, this would yield an observable net displacement only if there is a site-preference of substitution. In this case, any observed displacement would not only be in evidence of defect clustering, but would further provide insights into local coordination preferences.

## II. Computational Procedure

Selected defect structures, all containing one oxygen interstitial and zero to three Sn atoms, substituting for In at nearest and next-nearest sites, were geometry optimized using the first-principles density functional theory (DFT). All calculations were performed in the generalized gradient approximation (GGA)<sup>8,9</sup> of DFT using the VASP software.<sup>10–13</sup> Defect structures were represented within a single cubic unit cell of bixbyite containing 80 atoms ( $\text{In}_{32}\text{O}_{48}$ ), i.e.,  $\text{Sn}_{\text{In}}$ ,  $\text{O}_i$ , and  $(2\text{Sn}_{\text{In}} \cdot \text{O}_i)$  defects are represented by unit cells of stoichiometry  $\text{Sn}_1\text{In}_{31}\text{O}_{48}$ ,  $\text{In}_{32}\text{O}_{49}$ , and  $\text{Sn}_2\text{In}_{30}\text{O}_{49}$ , respectively.

All atomic positions in the unit cell were relaxed, while the dimensions of the cell were held fixed to those obtained in a separate bulk calculation (10.34 Å to be compared with 10.117 Å experimentally).<sup>5</sup> The constraint on the cell dimensions is applied here as an approximate representation of the strain because of the surrounding crystal.

Integrations over the Brillouin zone were performed on a  $2 \times 2 \times 2$  grid of k points. Valence as well as semi-core bands were expanded in a plane wave basis with a cut off at 300 eV. Core electrons were represented using Vanderbilt ultrasoft pseudopotentials.<sup>14,15</sup> In order to ascertain the degree of error because of finite energy cutoff on the computed quantities of interest to this work (defect energy differences and oxygen interstitial position), selected structures were recomputed using a 400 eV cutoff. While the increased cutoff resulted in changes in absolute energies of about 0.06 eV, changes in defect energy differences were found to be marginal (<0.01 eV). An increase of the k-point density had a similarly small effect on defect energy differences. For example, the defect energy difference of Sn substituting at an In b site and a d site was found to be 0.0847 and 0.0844 eV with 300 and 400 eV cutoffs, respectively. The same defect energy difference computes to 0.0843 eV (at 300 eV cutoff) when the k-point grid is increased to  $4 \times 4 \times 4$ . The discussion of our results is based entirely on defect energy differ-

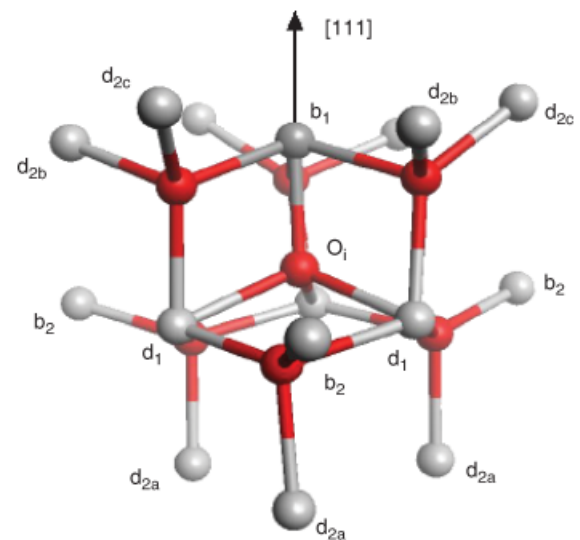


**Fig. 2.** (in color online) Local coordination geometry around interstitial oxygen ( $\text{O}_i$ ) in  $\text{In}_2\text{O}_3$  with first and second shell cation positions labeled by Wyckoff type (b or d) and shell index (in subscript) with respect to  $\text{O}_i$  (cf. text). Cation sites without label are related to labeled sites through the threefold rotation axis along [111]. Oxygen atoms and In/Sn cation positions are colored dark gray (red) and light gray, respectively.

ences that are (because of cancellation of errors) much less sensitive to the approximations made in this work. We quote here, for reference only, the absolute formation energy of a  $(2\text{Sn}_{\text{In}} \cdot \text{O}_i)^{\times}$  defect cluster in  $\text{In}_2\text{O}_3$ , which computes to +1.7 eV in our model; this is likely to be an overestimation because of periodic cluster-cluster interactions.

We denote cation positions where Sn substitutes for In by their Wyckoff type (b or d) and, via a numeric index, whether located in the first or second cation coordination shell of the interstitial. Thus, as Fig. 2 illustrates, we have four cations in the first shell: one b site (denoted  $b_1$ ) and three d sites (denoted  $d_1$ ). In the second shell, we have three b sites (denoted  $b_2$ ) and nine d sites, which, in sets of three, are symmetry related (we denote these sets collectively as  $d_2$  and separately as  $d_{2a}$ ,  $d_{2b}$ , and  $d_{2c}$ ).

## III. Results and Discussion

In Table I, we list the calculated defect energy as well as the projected position of the interstitial onto the 16c axis for defect clusters of varying stoichiometry (number of Sn atoms around  $\text{O}_i$ ) and the relative position of  $\text{Sn}_{\text{In}}$ . Defect energies are given relative to the most stable arrangement with the same number of  $\text{Sn}_{\text{In}}$  atoms to provide an indication of the relative preference (and thus likelihood of observation) between clusters of different structural configurations of the same stoichiometry; we stress that no inferences about the relative stability between clusters of different stoichiometry should be made from these energies. The projected position of the interstitial in Table I is calculated as  $(x+y+z)/3$  where  $x$ ,  $y$ , and  $z$  are the fractional lattice coordinates of  $\text{O}_i$  after full relaxation. This projection is the most appropriate value for comparison with the experimental diffraction result, which measures an average of symmetry-equivalent configurations. For convenience, the projected position in Table I has also been expressed in absolute terms relative to the experimental position  $x = y = z = 0.091(1)$  (this is the interstitial position of highest confidence, reported in González *et al.*<sup>7</sup> for an oxidized 9 at.-%ITO sample).

### (1) Interstitial Position

For an isolated oxygen interstitial  $\text{O}_i$ , we find the calculated projected position at  $x = y = z = 0.110$  reasonably close (0.11 Å)

**Table I.** Oxygen Interstitial ( $O_i$ ) Position (Projected Onto the [111] Axis; cf. Text), Calculated for Selected Clusters Containing up to Three Sn in the First and Second Coordination Shell

Cluster	Sn sites	Relative energy (eV)	Projected $O_i$ position	
			$x = y = z$ (lattice units)	Distance to exp. position ( $\text{\AA}$ )
$O_i^\times$	Nil	0.00	0.110	0.34
$[Sn \cdot O_i]^\times$	$b_2$	0.00	0.105	0.25
	$d_1$	0.03	0.098	0.12
	$d_2^\dagger$	0.13–0.16	0.107–0.108	0.29–0.30
	$b_1$	0.19	0.111	0.36
$[2Sn \cdot O_i]^\times$	$d_1d_1$	0.00	0.091	0.00
	$b_2b_2$	0.00	0.104	0.23
	$b_1d_1$	0.25	0.105	0.25
	$d_2d_2^\dagger$	0.33–0.35	0.106–0.109	0.27–0.32
$[3Sn \cdot O_i]^\times$	$b_2b_2b_2$	0.00	0.104	0.23
	$d_1d_1b_2$	0.13	0.094	0.05
	$d_1d_1d_1$	0.16	0.084	–0.13
	$b_1d_1d_1$	0.35	0.078	–0.23
	$d_2d_2d_2^\dagger$	0.50–0.63	0.107–0.109	0.29–0.32
Experiment	—	—	0.091 (1)	—

<sup>†</sup>Energy and positional ranges are based on a selection of three configurations. Relative defect energies are with respect to the most stable cluster of the same stoichiometry. The experimental interstitial position is taken from González *et al.*<sup>7</sup> for 9 at. % ITO sample. ITO, indium-tin oxide.

to the ideal position at 0.116 and significantly distant (0.34 Å) from the experimental position at 0.091. This reveals that the displacement of the interstitial observed experimentally is not an intrinsic property of the interstitial, and is thus most likely because of clustering with Sn. This is evident in the series of clusters ( $nSn \cdot O_i$ )<sup>×</sup> with one to three Sn substituents at the nearest d-type cation site, that is, clusters in Table I with Sn-site configurations  $d_1$ ,  $d_1d_1$ , and  $d_1d_1d_1$ . For these, we find the interstitial position to be increasingly displaced toward smaller values: 0.098, 0.091, 0.084 lattice units, respectively. The apparent excellent agreement with the experiment of the calculated position ( $x = y = z = 0.091$ )<sup>7</sup> for the ( $2Sn \cdot O_i$ )<sup>×</sup> cluster with  $d_1d_1$ -configuration is perhaps fortuitous; conservatively, we would be inclined to accept calculated distances of below 0.15 Å from the observed position, and thus all three configurations ( $d_1$ ,  $d_1d_1$ , and  $d_1d_1d_1$ ) as not in disagreement with the experiment. Looking now at Sn substitution at the nearest b site ( $b_1$ ), we observe a pull of the interstitial toward the b site and thus away from the plane of d sites and the experimental position. This can be seen in Table I by contrasting displacements between the following pairs of defect clusters (as characterized by their Sn-site occupations): nil versus  $b_1$  and  $d_1$  versus  $b_1d_1$ . In these two cases, the additional Sn atom at the  $b_1$  site results in a displacement to larger  $x = y = z$ , by 0.02 and 0.13 Å, respectively. Thus,  $b_1$  occupation is clearly not compatible with the experimental position. Substitutions in the second shell at  $d_2$  and especially at  $b_2$  sites lead to displacements to smaller  $x = y = z$ ; however, these displacements are small in contrast to those achieved by  $d_1$  substitutions. In the set of second shell substitutions investigated by us, the largest displacement through second shell substitution alone brought the interstitial to  $x = y = z = 0.104$ , which is still at a distance of 0.23 Å from the experimental position. In summary, Table I shows that only Sn substitution at  $d_1$  sites results in  $O_i$  displacements toward the plane of three nearest d sites to an extent consistent with experimental observation.

## (2) Substitution Site Preference

We now discuss the relative energies of defect clusters in Table I with a particular focus on substitution preference for Sn at cation b versus d sites. Experimental data indicates a strong preference of Sn to substitute at the b site rather than the d site.<sup>6,7,16</sup> How does this b preference come about and how is it reconcil-

able with our conclusion that the observed  $O_i$  position is clustered with d-site Sn?

In the absence of nearby interstitial oxygen, the energy of an  $Sn_{In}^\times$  substitutional defect at a cation b site is calculated to be more stable by 0.08 eV than at the d site. This result is in qualitative agreement with earlier first-principles FLMTO calculations by Myrazov and Freeman,<sup>17</sup> who found a 0.05 eV preference for the b site. Preference for the b site, however, is in disagreement with our earlier empirical shell model calculations, which concluded equal preference to within calculational error.<sup>18</sup> As we find  $Sn_{In}$  to be clustered with  $O_i$ , it is perhaps more relevant to enquire how b- versus d-site preferences play out in the vicinity of interstitial oxygen. Comparison of the energies in Table I between three pairs of clusters (as characterized by their Sn-site occupations),  $d_2$  versus  $b_2$ ,  $d_2d_2$  versus  $b_2b_2$ , and  $d_2d_2d_2$  versus  $b_2b_2b_2$ , reveals a b preference of 0.13, 0.17, and 0.17 eV per b/d-pair, respectively; thus, b-site preference in the second shell around  $O_i$  appears to be enhanced compared with the preference calculated for isolated  $Sn_{In}$ . Similarly, we contrast b and d sites in the first shell around an interstitial. Comparing clusters with sites at  $d_1$  versus  $b_1$ ,  $d_1d_1$  versus  $b_1d_1$ , and  $d_1d_1d_1$  versus  $b_1d_1d_1$ , all differing by a single  $Sn_{In}$  at  $d_1$  moved to  $b_1$ , illustrates a reversed site preference: in the first cation shell of an interstitial, substitution at the  $d_1$  site is preferred over the  $b_1$ -site by 0.16, 0.25, and 0.19 eV, for the three examples, respectively. Finally, we discuss shell preference or the relative energetics of first-shell versus second-shell Sn substitution where we focus on  $d_1$  and  $b_2$  sites, the favored positions in each shell. Comparison of  $d_1$  versus  $b_2$ ,  $d_1d_1d_1$  versus  $d_1d_1b_2$ , and  $d_1d_1$  versus  $b_2b_2$  reveals marginal preferences for the second shell of below 0.03 eV, but also note the transition  $d_1d_1d_1$  to  $b_2b_2b_2$ , which leads to a substantial gain of 0.16 eV (or 0.05 eV per  $d_1/b_2$ -pair). We rationalize this particular gain as being driven by the mutual repulsion of three (formally net positive) Sn dopants crowded together in the first shell. It is thus very plausible that the distribution of Sn dopants between the first and second shell is less determined by shell preferences and is instead driven by the need to minimize repulsion between Sn dopants. This is in qualitative agreement with our earlier shell model calculations.<sup>4,8</sup> These site and shell preferences also provide insights into what may appear to be a conundrum in the experimental data: interstitial displacement points toward d site Sn occupation; yet, an overall preferential Sn substitution at the b site is observed.<sup>6,7,16</sup> The calculated d-site preference in the first shell and b preference in

the second shell to an interstitial, in conjunction with the fact that second shell sites are more numerous, yields a consistent resolution to this conundrum.

#### IV. Summary

Rietveld analysis of X-ray and neutron diffraction data of ITO reveals that interstitial oxygen is significantly displaced from the ideal fourfold position.<sup>7</sup> First-principles density functional calculations carried out in this work show that these displacements are plausible only when Sn dopants are located at the d site nearest to the interstitial. This means that the experimentally observed displacements are direct structural evidence for the clustering of interstitial oxygen with Sn dopants, as postulated by the Frank and Köstlin model.<sup>3</sup>

#### References

- <sup>1</sup>D. S. Ginley and C. Bright, "Transparent Conducting Oxides," *MRS Bull.*, **25** [8] 15 (2000).
- <sup>2</sup>C. G. Granqvist and A. Hultåker, "Transparent and Conducting ITO Films: New Developments and Applications," *Thin Solid Films*, **411**, 1–5 (2002).
- <sup>3</sup>G. Frank and H. Köstlin, "Electrical Properties and Defect Model of Tin-Doped Indium Oxide Layers," *Appl. Phys. A*, **27**, 197 (1982).
- <sup>4</sup>O. Warschkow, D. E. Ellis, G. B. González, and T. O. Mason, "Defect Cluster Aggregation and Non-Reducibility in Tin-Doped Indium Oxide," *J. Am. Ceram. Soc.*, **86**, 1707–11 (2003).
- <sup>5</sup>M. Marezio, "Refinement of the Crystal Structure of  $In_2O_3$  at Two Wavelengths," *Acta Crystallogr.*, **20**, 723–8 (1966).
- <sup>6</sup>G. B. González, J. B. Cohen, J. H. Hwang, T. O. Mason, J. P. Hodges, and J. D. Jorgensen, "Neutron Diffraction Study of the Defect Structure of Indium-Tin-Oxide," *J. Appl. Phys.*, **89**, 2550–5 (2001).
- <sup>7</sup>G. B. González, T. O. Mason, J. P. Quintana, O. Warschkow, D. E. Ellis, J. P. Hodges, and J. D. Jorgensen, "Defect Structure Studies of Bulk- and Nano-Indium-Tin-Oxide," *J. Appl. Phys.*, **96**, 3912–20 (2004).
- <sup>8</sup>J. P. Perdew, "Unified Theory of Exchange and Correlation Beyond the Local Density Approximation"; p. 11 in *Electronic Structure of Solids '91*, Edited by P. Ziesche and H. Eschrig. Akademie Verlag, Berlin, 1991.
- <sup>9</sup>J. P. Perdew, J. A. Chevary, S. H. Vosko, K. A. Jackson, M. R. Pederson, D. J. Singh, and C. Fiolhais, "Atoms, Molecules, Solids and Surfaces: Applications of the Generalized Gradient Approximation for Exchange and Correlation," *Phys. Rev. B*, **46**, 6671–87 (1992).
- <sup>10</sup>G. Kresse and J. Hafner, "Ab Initio Molecular Dynamics for Liquid Metals," *Phys. Rev. B*, **47**, 558–61 (1993).
- <sup>11</sup>G. Kresse and J. Hafner, "Ab initio Molecular Dynamics Simulation of the Liquid-Metal-Amorphous-Semiconductor Transition in Germanium," *Phys. Rev. B*, **49**, 14251–69 (1994).
- <sup>12</sup>G. Kresse and J. Furthmüller, "Efficiency of Ab-Initio Total Energy Calculations for Metals and Semiconductors using a Plane-Wave Basis Set," *Comput. Mater. Sci.*, **6**, 15–50 (1996).
- <sup>13</sup>G. Kresse and J. Furthmüller, "Efficient Iterative Schemes for Ab Initio Total Energy Calculations Using a Plane-wave Basis Set," *Phys. Rev. B*, **54**, 11169–85 (1996).
- <sup>14</sup>D. Vanderbilt, "A Self-consistent Pseudopotential in a Generalized Eigenvalue Formalism," *Phys. Rev. B*, **41**, 7892–5 (1990).
- <sup>15</sup>G. Kresse and J. Hafner, "Norm-conserving and Ultrasoft Pseudopotentials for First Row and Transition Elements," *J. Phys.: Condens. Matter*, **6**, 8245–57 (1994).
- <sup>16</sup>N. Nadaud, N. Leequeux, M. Nanot, J. Jové, and T. Roisnel, "Structural Studies of Tin-Doped Indium Oxide (ITO) and  $In_4Sn_3O_{12}$ ," *J. Solid State Chem.*, **135**, 140 (1998).
- <sup>17</sup>O. N. Myrazov and A. J. Freeman, "Electronic Band Structure of Indium Tin Oxide and Criteria for Transparent Conducting Behaviour," *Phys. Rev. B*, **64**, 233111 (2001).
- <sup>18</sup>O. Warschkow, D. E. Ellis, G. B. González, and T. O. Mason, "Defect Structures of Tin-doped Indium Oxide," *J. Am. Ceram. Soc.*, **86**, 1700–6 (2003). □